JOURNAL OF PROPULSION AND POWER
Vol. 27, No. 3, May–June 2011

Gas Turbine Combustor Sector Flow Structure

B. S. Mohammad* and S. M. Jeng†
University of Cincinnati, Cincinnati, Ohio 45220

DOI: 10.2514/1.B34114

Detailed flow structure investigations on a single annular combustor sector are reported using laser Doppler velocimetry and particle image velocimetry. The single annular combustor sector comprises a swirl cup with counter-rotating coaxial radial inlet swirlers, film cooling strips, and primary and secondary dilution jets. The mean flow results demonstrate the presence of the four jets and their wake regions. High-turbulence activities are generated in all shear layers and mixing regions. Sequential reacting-flow images show that heat release takes place in such regions, provided that there is an adequate local fuel/air ratio. The three-dimensional shape of the central recirculation zone is reconstructed through a set of several offcenter particle image velocimetry measurements. The three-dimensional shape of the central recirculation zone reveals the strong influence of the confinement on the shape of the central recirculation zone. The width-to-breadth ratio of the reconstructed central recirculation zone is similar to that of the confinement (85%). Instantaneous particle image velocimetry results reveal that the primary jets control the structure of the primary and the secondary combustor regions. The wake regions and central recirculation zone all maintained their absolute size at different pressure drops.

Nomenclature

R	=	flare exit radius
V	=	total velocity, $\sqrt{(V_a^2 + V_r^2)}$
Va	=	axial velocity component
Vr	=	radial velocity component
X, Y, Z	=	Cartesian coordinate system with the origin defined at the flare center
$\Delta P/P$	=	pressure-drop percentage

I. Introduction

THE requirements of low emissions and stable combustion are given the first priority in the development and design of gas turbine combustors. Combustor flow dynamics (also referred to as aerodynamics) play a vital rule in stability, emissions, and dynamics characteristics of gas turbine combustors. Researchers working in the field of combustion are in continuous need to understand the complex flow behavior in realistic combustion chambers to be able to resolve combustion challenges.

Swirling flow is commonly used in gas turbine combustors, primarily for flame anchoring. The idea depends on the generation of a central recirculation zone (CRZ) that improves mixing and the blowout limits [1–3]. The swirling flow, of sufficient strength, induces small scale instantaneous eddies in the flowfield, in the vicinity of the CRZ, and such eddies were shown to have very strong influence on the orientation of the reaction zone [4]. The swirl cup was introduced as a unique device to prepare the air/fuel mixture. Many studies were conducted on counter-rotating swirl cup [5–11]. Mongia [12] discussed in details the bench mark experiments that were conducted on the swirl cup and he compared the measurements to the computational fluid dynamics results. Yet, none of the experimental investigations were conducted on realistic combustion chambers. The geometries were simple rectangular geometries with no primary and secondary dilution jets. In reality, the interaction between the swirling flow and primary dilution jets significantly affects the flowfield structure and dynamics and emissions. The single annular combustor (SAC) sector under investigation was subjected to extensive experimental investigation at the University of Cincinnati Combustion Research Laboratory. The combustion dynamics spectrum was established, and a novel method for combustion dynamics diagnostic was developed [13]. The technique enables identification of the mode and the location of the combustion dynamics within the combustor. The flow structure control via perturbation of the primary jets and geometrical modifications was also studied extensively [14,15].

The current study is conducted under isothermal flow conditions. The experimental setup is very challenging, and reacting-flow experiments are very expensive, if possible. The literature (for example, [16–22]) shows that the differences between isothermal and reacting flow are located in the primary zone close to the swirler exit. However, the secondary and dilution zones have several similarities: mainly, the turbulence levels in these regions are very similar [23].

In the current research, measurements are conducted on a SAC sector, also known as a fuel-rich dome combustor. The SAC resembles a realistic gas turbine combustor. The SAC comprises a counter-rotating swirl cup, combustion dome with cooling holes and slots, inner and outer passage to provide cooling and dilution air, liner with variable cross section with cooling strips, and holes to provide primary and secondary dilution jets. The liner contracts toward the end to allow fitting of the combustor to the turbine nozzle ring. Laser Doppler velocimetry (LDV) and particle image velocimetry (PIV) measurements are conducted to delineate the flowfield structure and to study the interaction between the swirling flow and the dilution jets. In addition, the shape of the CRZ in 3-D is studied by conducting PIV measurements on several planes located off the SAC sector centerline plane. The PIV data are imported to CAD software to enable reconstruction of the CRZ in 3-D. The effect of the pressure drop on the flow structure is also presented. Finally, instantaneous PIV is used to understand the mixing process and to study the effect of primary dilution air on the flow structure of different combustor zones.

II. Experimental Setup, Procedure, and Test Conditions

A. Swirl Cup and SAC Combustor

The counter-rotating coaxial radial swirl-cup arrangement is shown in Fig. 1. The inner swirler is connected to a venturi tube, as shown in Fig. 1. The area ratio of the secondary to primary swirler is

Presented as Paper 2010-579 at the 48th AIAA Aerospace Sciences Meeting, Orlando, FL, 4–7 January 2010; received 13 September 2010; revision received 10 November 2010; accepted for publication 16 November 2010.

*Ph.D., Aerospace Engineering and Engineering Mechanics, 745 Baldwin Hall, Room ML 70. Student Member AIAA.

†Professor, Aerospace Engineering and Engineering Mechanics, 745 Baldwin Hall, Room ML 70. Member AIAA.

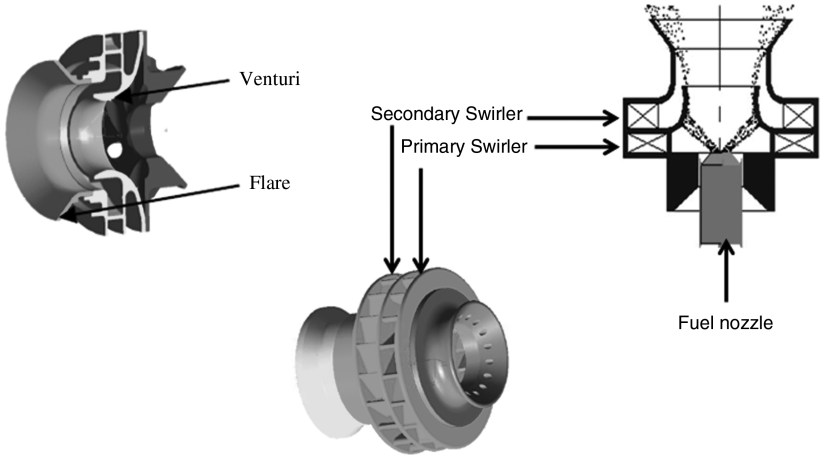

Fig. 1 Typical swirl-cup arrangement with coaxial counter-rotating swirlers.

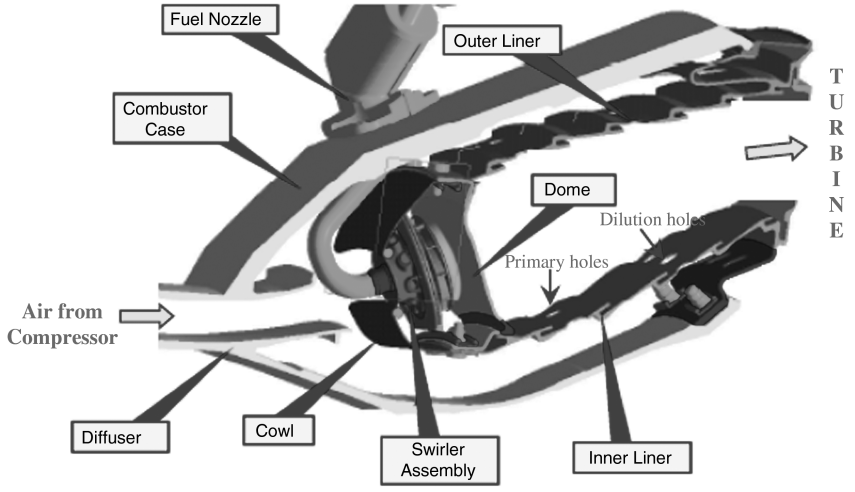

Fig. 2 Typical SAC combustor.

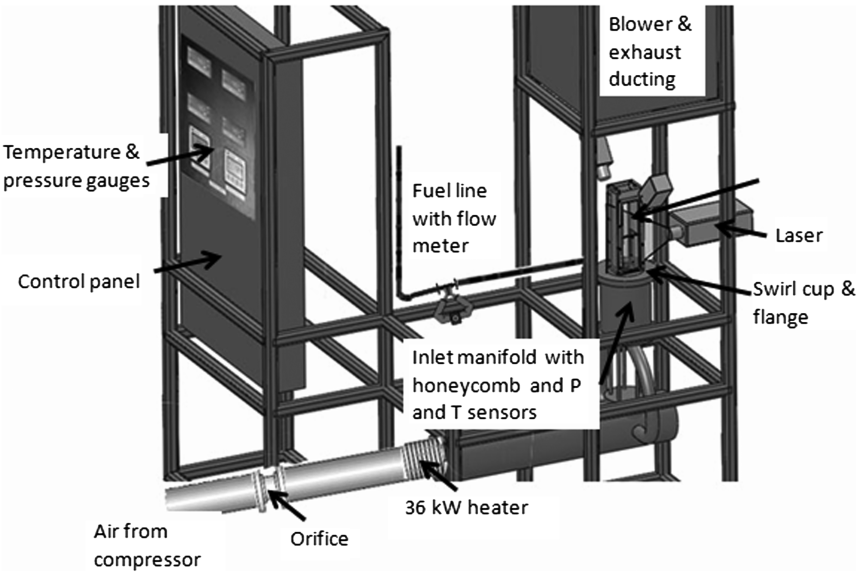

Fig. 3 Experimental facility.

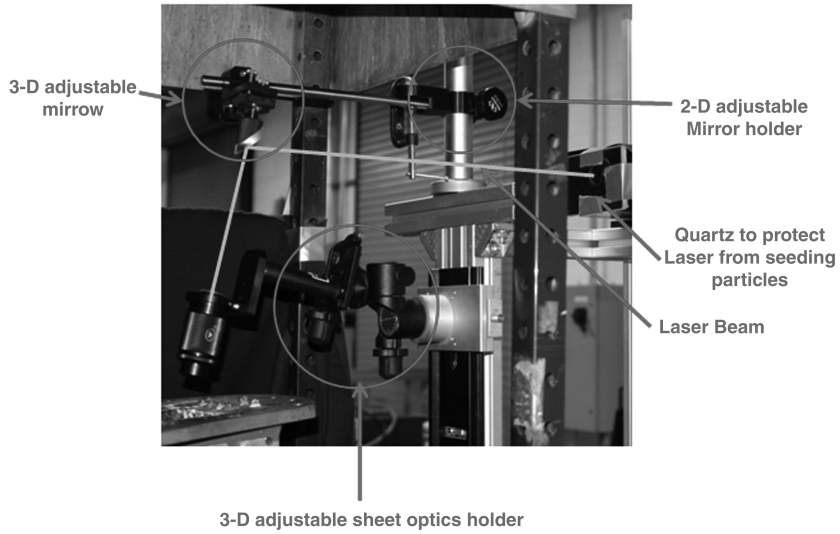

Fig. 4 Optical arrangement for locating the laser sheet at the desired measurement plan.

greater than 1. The secondary swirler is connected to a conical flare. The effective area of the swirl cup is 400 mm^2.

The SAC sector used is similar, in construction, to the combustor shown in Fig. 2. The sector comprises two side quartz windows, primary and secondary dilution jets, eight film cooling strips on each side, combustion dome with cooling slots, inlet cowl, and inlet diffuser.

B. Experimental Facility

A schematic of the laser diagnostic facility at the University of Cincinnati Combustion Research Lab is presented in Fig. 3. A 203 mm polyvinyl chloride (PVC) pipe is used as a manifold. A honeycomb inside the manifold provides uniform flow to the test section. The SAC assembly is mounted on a flange above the PVC. Pressure sensor and thermocouples are mounted inside the manifold

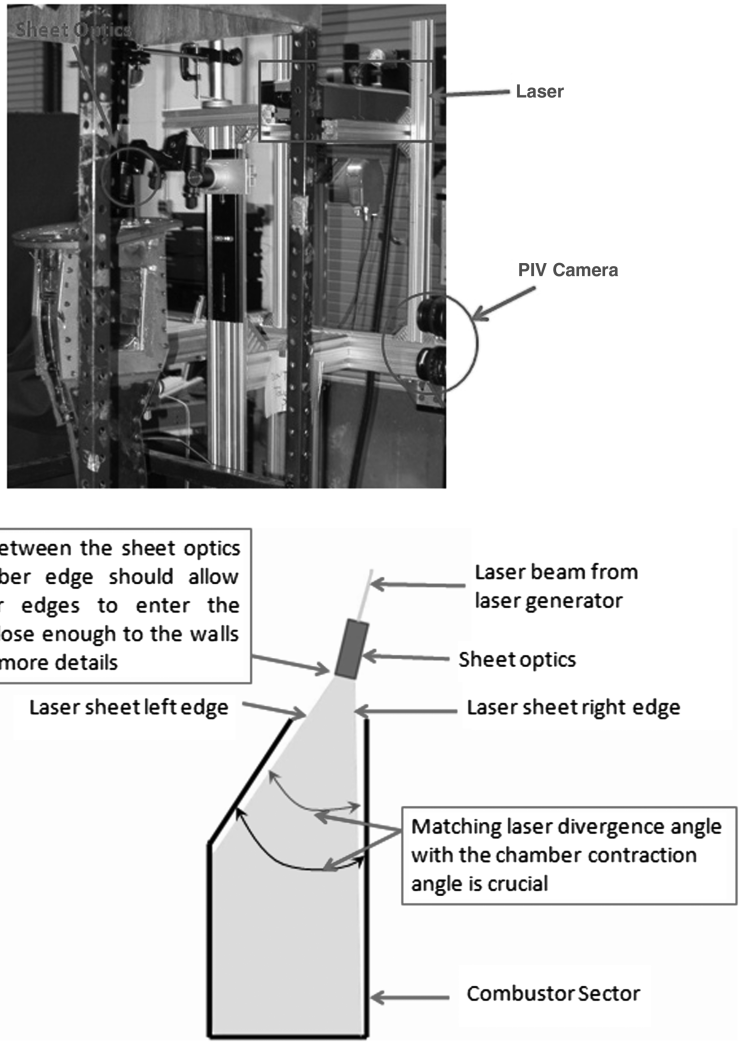

Fig. 5 PIV setup on the rig.

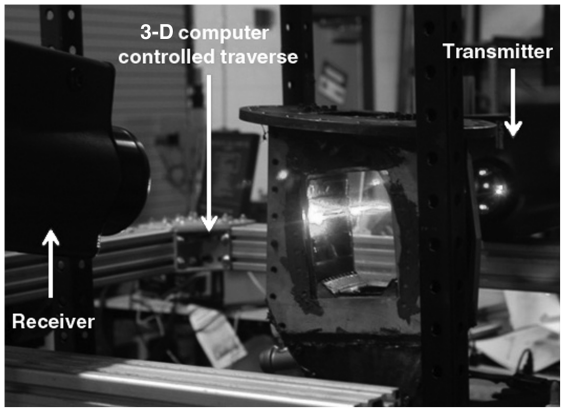

Fig. 6 LDV setup on the test rig.

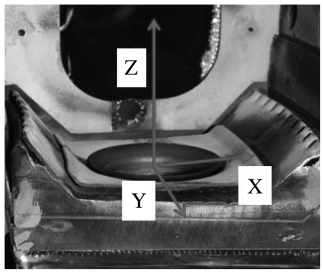

Fig. 7 Measurement coordinate system.

for monitoring of pressure and temperature at the test-section inlet. Air enters the manifold through a 50 mm pipe that can provide pressurized air up to 1 kg/s at 6.8 bar. An atomizer generating olive oil seeding particles (1–5 μm) is connected to the manifold through a seeding port. A blower and an exhaust system are mounted above the test section to collect aerosols.

C. Diagnostics

Flowfield measurements are conducted using PIV and LDV. The PIV system is supplied by Lavision, Inc. The system includes two 1376×1040 pixel 12-bit Lavision imager intensified charge-coupled device (CCD) cameras and two 120 mJ 15 Hz pulse Nd-Yag lasers that are synchronized with CCD cameras. A mirror is used to get the laser beam to the sheet optics and provide the laser sheet at the correct measurement plane from the SAC sector exit, as depicted in Fig. 4. Both cameras are placed on the top of one another to extend the measurement volume (see Fig. 5). Both cameras are placed perpendicular to the laser sheet. The setup is a real challenge, since the exit port of the SAC sector has reduced width to fit the turbine nozzle ring. Figures 4 and 5 are self-explanatory of the complexity of the PIV setup. The setup is accomplished through the following steps:

1) A proper choice of the laser sheet optics is important in order to generate a laser sheet with a spread angle close to the SAC sector nozzle angle, as illustrated in Fig. 5.

2) Sheet optics should be placed at the correct spot from the sector exit. The correct spot is the one that enables both laser edges to enter the chamber without interference with the walls. However, the laser edges has to be as close as possible to the walls to enable capturing as much detail as possible.

3) The final, and most difficult, step is to locate the laser sheet in the correct measurement plane. This step needs experience and patience, since rotation of the sheet optics should be accompanied with the mirror adjustment to have the laser beam hit the splitter in the correct spot.

But if the mirror angle changes, then step 2 should be repeated. Steps 2 and 3 are repeated simultaneously until the laser sheet covers as much as possible from the combustor flowfield and is located in the correct measurement plane.

The two-component LDV measurements are conducted using an Artium Technologies, Inc., system. The system uses two diode-pumped solid-state lasers as the light source, which does not require air or water cooling. The system comprises a transmitter, a receiver, two digital signal processors, and a computer. The 500 mm focal length transmitter and 300 mm focal length receiver are mounted on a computer-controlled traverse, as depicted in Fig. 6.

D. Test Conditions and Data Acquisition

The measurements coordinate system is defined such that the axial direction of the swirler is designated as the Z direction, with the zero set at the flare exit. The X direction is perpendicular to the Z direction and in the dilution air jet plane. The origin of this coordinate system is located at the center of the swirler exit. The coordinate system is shown in Fig. 7. Experiments are carried out for isothermal flow conditions under ambient pressure and temperature of 70 ± 1°F. Pressure-drop measurements are accurate to within $\pm 0.1\%$.

LDV measurements are conducted at total pressure drop of 4.9% (or the total pressure loss in the combustor). Data count is typically more than 7000 for the green laser (radial component of the velocity) and 3000 for the blue laser (axial component of the velocity). The uncertainty in the mean velocity is within 0.1–0.3 m/s.

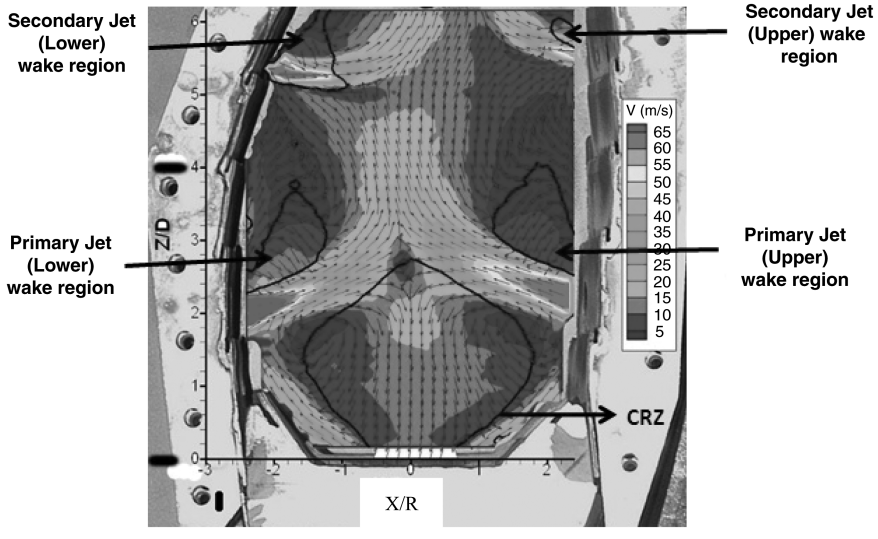

Fig. 8 SAC combustor total velocity contours using LDV at $\Delta P/P = 4.9\%$.

PIV measurements are conducted in the X–Z plane passing by the SAC center ($Y = 0$) at pressure-drop ratios of 7.6 and 4.3%, respectively, to study the effect of pressure drop on the flowfield. Several PIV measurements are also conducted offcenter to study the flowfield behavior offcenter and to help construct the CRZ in 3-D. Namely, measurements are conducted in the X–Z plane at Y distances of $0.66R$, $1.12R$, and $1.32R$, respectively.

The authors used 50, 75, 100, 150, and 200 images in processing the PIV images. The best resolution and minimum change in average are noted as the number of images approaches 150 images. The error in average is known to be the standard deviation divided by the number of images to the power of 0.5. Consequently, the authors increased the number of images to 200 in order to bring the error to a minimum while maintaining reasonable time in acquiring and processing the data.

The laser sheet is focused in the primary zone and close to the primary jets (region of high gradients). As reported in the literature, as long as a minimum of 10 seeding particles occur within the interrogation area, then the removal of the spurious vectors using the deviation from the local median (and replacing either by vectors corresponding to the second-, third-, or fourth-highest correlation peak) should result in a typical uncertainty of 5–10% [24].

III. Results and Discussions

A. LDV Results

Figure 8 presents the total velocity contours in the vertical plane passing by the combustor centerline. As the flow emanates from the swirl cup it expands and flow reversals occur and a typical CRZ is set, as shown in Fig. 8. The black contours are contours of zero axial velocity. As mentioned earlier, the combustor comprises a set of primary and secondary dilution holes. There are four dilution jets in the measurement plane. The upper left jet is shooting down at an angle. The other three jets have horizontal exits. The four are clearly identified from their high total exit velocity, as shown in Fig. 8. The jet trajectories are not radial, due to the momentum imposed from the main flow on the jets. This is a typical jet in crossflow configuration. As the dilution jets mix with the main flow, we note the formation of four jet wake regions. The size of the primary dilution jet wake regions are more than twice the secondary dilution jet wake regions (due to the higher jet momentum).

The expanding jet velocity on the negative x direction (close to the dome edge) is larger than that on the positive x direction because of the asymmetry in the dome expansion angle. As the main flow proceeds downstream it interacts with the primary dilution jets and the CRZ is closed, as depicted in Fig. 8.

The total velocity contours reveals that the high-speed regions are the dilution jets and the jet mixing regions. The remaining regions of the combustor are relatively low-speed regions.

Figures 9 and 10 demonstrate the root-mean-square values of the axial and radial velocities, respectively. High-turbulence activities are noted in all jet regions (shear layer regions). However, the central region of the combustor, where the primary jets mix with the main flow, is the region of maximum turbulence activities. Such regions become very sensitive and susceptible to periodic oscillations. Indeed, while studying the SAC reacting-flow dynamics, the combustion research group at the University of Cincinnati noted the generation of such instabilities [13]. Also, during the SAC sector ignition, the same regions may even ignite before other regions, depending on the location of the ignition source (compare Figs. 10 and 11). The image is captured by a Phantom high-speed camera during ignition at 6600 frames per second.

Figure 12 shows a set of images captured sequentially while conducting reacting-flow experiments (burning propane). In this set, the fuel is being increased steadily from an equivalence ratio of 0.2 to 0.9. The blue color is an indication of reaction taking place (color of the CH radical). We note that the reaction initially takes place at the CRZ edge. As fuel increases, it progresses downstream and reaches the primary jet's lower boundary. Then it progresses to the primary jet's upper boundary. Then it reaches the secondary jet's upper and lower boundaries.

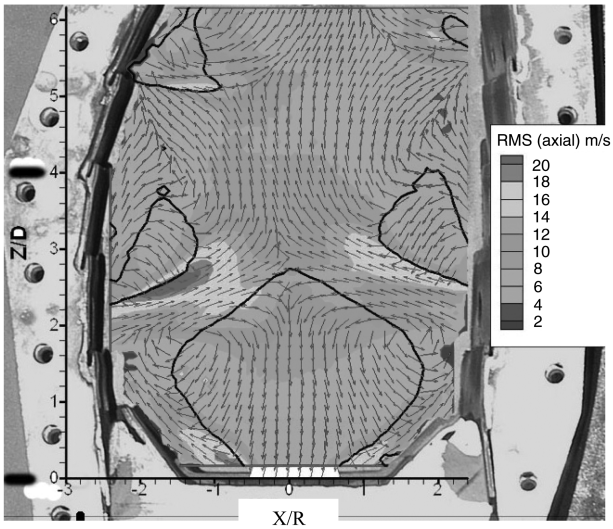

Fig. 9 Root mean square of the axial velocity.

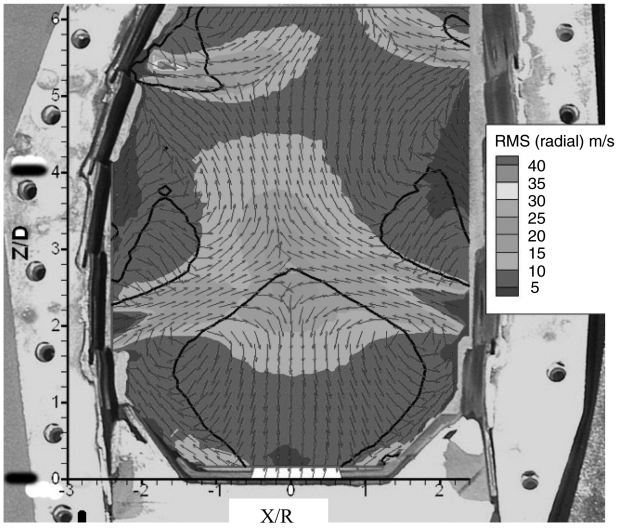

Fig. 10 Root mean square of the radial velocity.

B. PIV Results

PIV offcenter contours are not presented in this paper for reasons of brevity. The offcenter PIV measurements are analyzed and the edge of the CRZ is obtained at four vertical planes (centerline, $0.66R$, $1.12R$, and $1.32R$). The edge of the CRZ is then reconstructed in 3-D using Solidworks 2009, as depicted in Fig. 13. The dimensions of the CRZ are given in Fig. 14. The height of the CRZ is roughly constant and equal to $2.7R$. In the X direction the CRZ extends up to $1.6R$. However, in the Y direction the CRZ extends up to $1.3R$. The CRZ extends slightly over the size of the flare in the X direction, yet it extends significantly in the Y direction. This is mainly due to

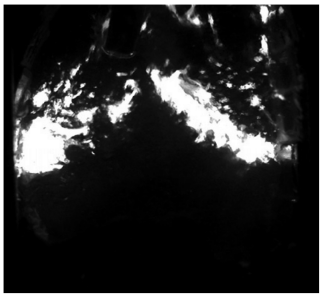

Fig. 11 SAC combustor during ignition.

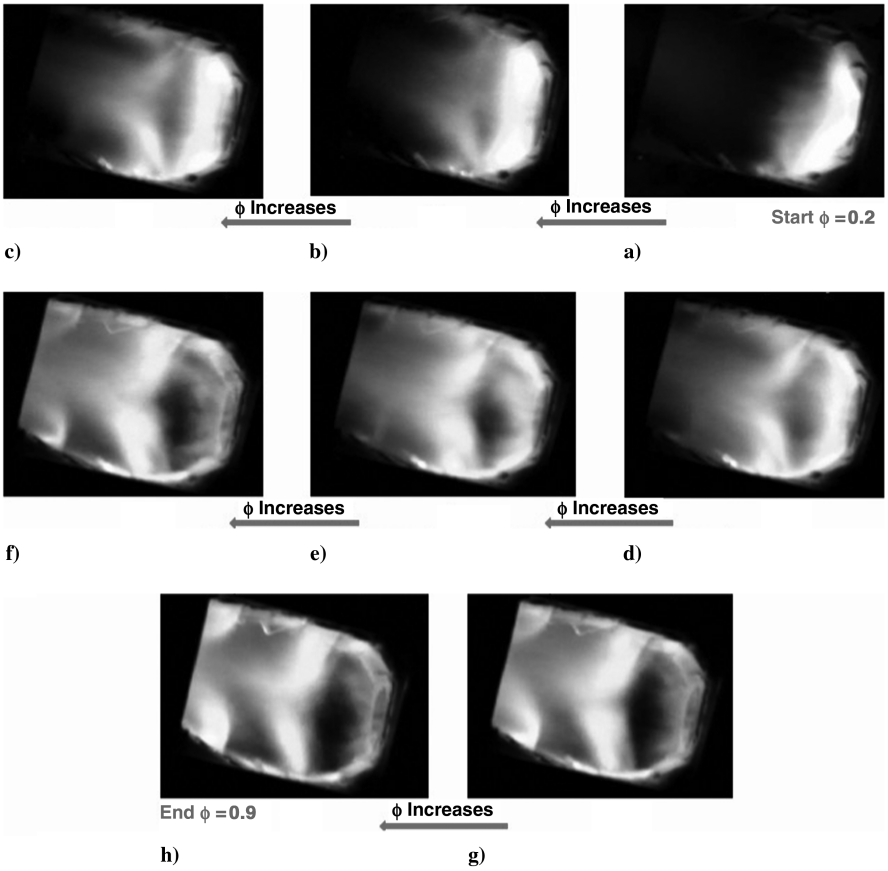

Fig. 12 Set of images showing progression of the reaction zone as the fuel is increased steadily from equivalence ratio of 0.2 to 0.9.

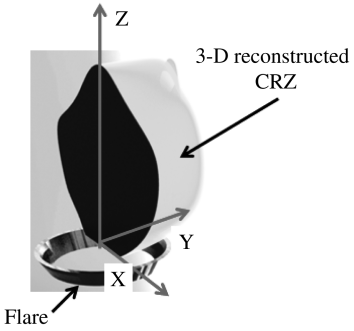

Fig. 13 Three-dimensional reconstructed CRZ over the flare.

confinement configuration. The SAC sector is not a square chamber. The primary zone of the SAC sector is illustrated with the dimensions in Fig. 15. The parameters b and w are the breadth and width at the centerline, respectively. The ratio of b/w is around 0.81. The ratio of the CRZ b/w ($1.3R/1.6R$) is around 0.85. It is worth noting that similar observations were concluded from the testing of the hardware in a square chamber (dump combustor) with a b/w ratio of 0.85 [25]. The results reveal the strong effect of the confinement on the shape of the CRZ.

Instantaneous PIV results are shown in Fig. 16. The results reveal the true behavior of the primary dilution jets. They also show the strong interaction and influence of the dilution jets on the flowfield structure. The dilution jets are in continuous up-and-down fluctuations. The instantaneous PIV results are classified into three scenarios, as depicted in Fig. 16. The first scenario is when both jets impinge. When this takes place, the flow is fairly symmetric, and around the combustor centerline a portion of the flow is going up and the other portion goes down toward the flare. The second scenario is when the right dilution jet is shooting up and at the same instant the left dilution jet is shooting down, as demonstrated in Fig. 16. At this point, the flowfield structure in the primary zone is dictated by the left dilution jet, which is shooting down and directly feeding the CRZ. On the contrary, the post-recirculation-zone structure is controlled by

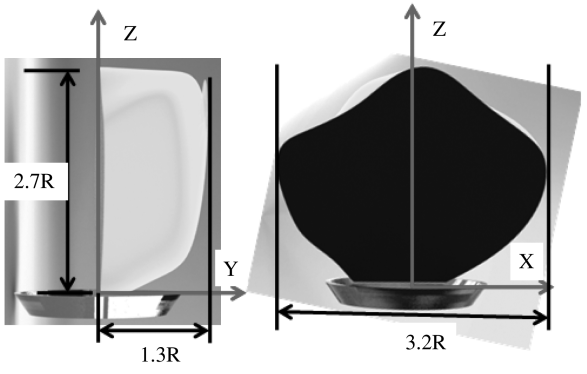

Fig. 14 Dimensions of the SAC sector CRZ.

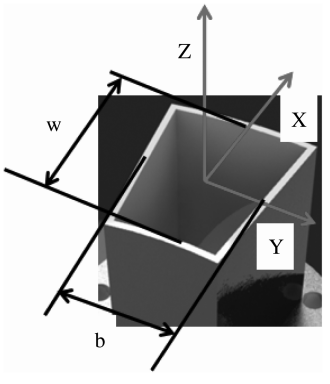

Fig. 15 SAC cross-sectional schematic in the primary zone.

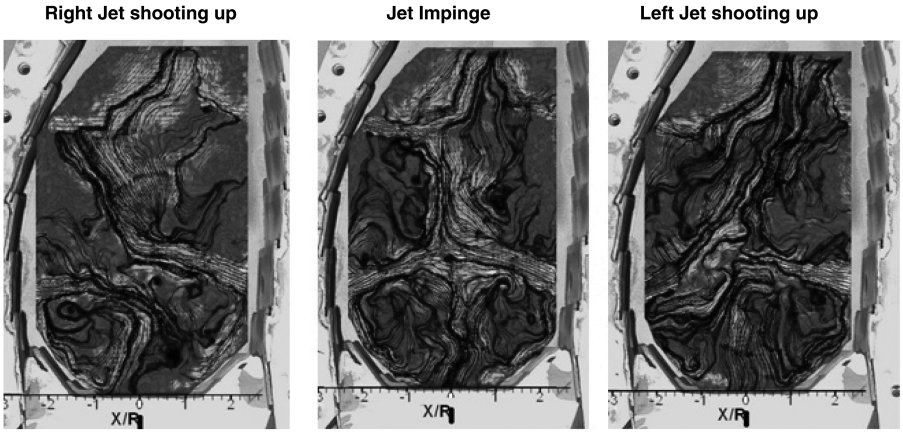

Fig. 16 Instantaneous PIV results.

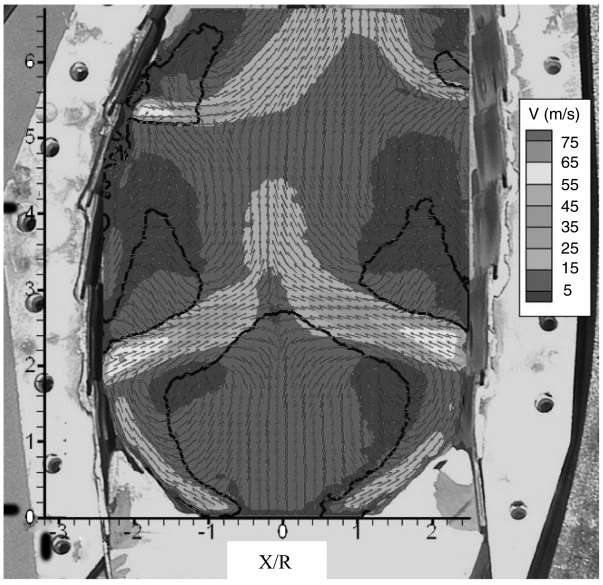

Fig. 17 Average flowfield using PIV at pressure drop of 4.3%.

the right dilution jet, which is shooting up and interacting strongly with the secondary-region flow. The third scenario is when the right dilution jet is shooting down and the left dilution jet is shooting up. This could be explained in a similar fashion to the second scenario. A separate detailed study on the possibility of using the primary-jet sensitivity to control the flow structure is presented in [15].

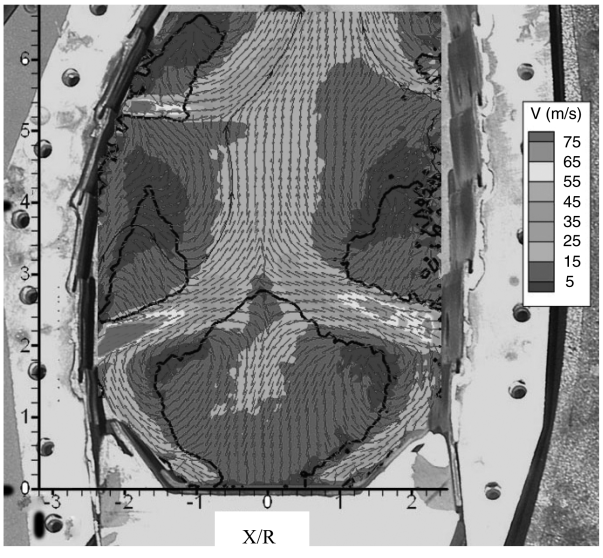

Fig. 18 Average flowfield using PIV at pressure drop of 7.6%.

Total velocity contours at pressure drops of 4.3 and 7.6% are presented in Figs. 17 and 18, respectively. The CRZ and all wake regions roughly maintained their absolute size. It is commonly known that the termination point of the CRZ is determined by the dilution jets. It is concluded that the flow structure is independent of the pressure drop. It is noteworthy that the left primary-jet wake region was found to continuously change in size with fuel injection, whereas the right primary-jet wake region was not dependent on fuel injection. Jet wake regions are ignition sources, and their sensitivity to different parameters may be a reason for generation of combustion dynamics.

IV. Conclusions

Complex flowfield structure in a realistic single cup combustor sector is successfully explored using LDV and PIV. The reacting-flow images show that the reaction propagation takes place along the edge of the CRZ and the edge of the primary and secondary dilution jets, depending on the local air/fuel equivalence ratio.

The CRZ is successfully reconstructed by conducting a set of PIV measurements at a set of parallel vertical planes located off the combustor center plane. Consequently, better understanding of the CRZ role in stabilizing the flame and igniting the mixture is possible. The 3-D shape of the CRZ reveals the strong influence of the confinement geometry on the 3-D shape of the CRZ. The ratio of major-to-minor axis is roughly 85%, which is similar to that of the confinement.

The role of the primary jets in dictating the flowfield in the dome region and the secondary region is assessed. The results suggest that the primary jets could be used effectively in controlling the combustor internal flowfield structure.

Pressure drop appears to have no influence on the flowfield structure at high Reynolds numbers. In other words, the sizes of the CRZ and jet wake regions are not influenced by the increase in pressure drop.

References

[1] Beer, J. M., and Chigier, N., *Combustion Aerodynamics*, Applied Science, London, 1972.

[2] Gupta, A. K., Lilley, D. G., and Syred, N., *Swirl Flows*, Abacus Press, Kent, England, U.K., 1984.

[3] Syred, N., and Beér, J. M., "Combustion in Swirling Flows: A Review," *Combustion and Flame*, Vol. 23, No. 2, 1974, pp. 143–201. doi:10.1016/0010-2180(74)90057-1

[4] Sadanandan, R., and Stöhr, M. M. W., "Simultaneous OH-PLIF and PIV Measurements in a Gas Turbine Model Combustor," *Applied Physics B (Lasers and Optics)*, Vol. 90, Nos. 3–4, 2008, pp. 609–618. doi:10.1007/s00340-007-2928-8

[5] Mongia, H. C., Al-Roub, M., Danis, A. E.-L. D., Johnson, A., Vise, S., Jeng, S. M., McDonell, V., and Samuelsen, G. S., "Swirl Cup Modeling Part 1," 37th AIAA/ASME/SAE/ASEE Joint Propulsion Conference

and Exhibit, AIAA Paper 2001-3576, Salt Lake City, UT, 2001.

[6] Hsiao, G., Mongia, H. C., and Atul, V., "Swirl Cup Modeling Part II: Inlet Boundary Conditions," 41st Aerospace Sciences Meeting and Exhibit, AIAA Paper 2003-1350, Reno, NV, 2003.

[7] Hsiao, G., and Mongia, H. C., "Swirl Cup Modeling Part 3: Grid Independent Solution with Different Turbulence Models," 41st Aerospace Sciences Meeting and Exhibit, AIAA Paper 2003-1349, Reno, NV, 2003.

[8] Cai, J., Fu, Y., Elkadi, A., Jeng, S., and Mongia, H., "Swirl Cup Modeling Part 4: Effect of Confinement on Flow Characteristics," AIAA Paper 2003-0486, 2003.

[9] Wang, S., Yang, V., Mongia, H., Hsieh, S., and Hsiao, G., "Modeling of Gas Turbine Swirl Cup Dynamics, Part V: Large Eddy Simulation of Cold Flow," 41st Aerospace Sciences Meeting and Exhibit, AIAA Paper 2003-0485, Reno, NV, 2003.

[10] Stevens, E. J., Held, T. J., and Mongia, H. C., "Swirl Cup Modeling Part VII: Partially-premixed Laminar Flamelet Model Validation and Simulation of a Single-cup Combustor with Gaseous N-heptane," 41st Aerospace Sciences Meeting and Exhibit, AIAA Paper 2003-488, Reno, NV, 2003.

[11] Stevens, E. J., Held, T. J., and Mongia, H. C., "Swirl Cup Modeling Part VIII: Spray Combustion in CFM-56 Single Cup Flame Tube," 41st Aerospace Sciences Meeting and Exhibit, AIAA Paper 2003-0319, Reno, NV, 2003.

[12] Mongia, H., "Perspective of Combustion Modeling for Gas Turbine Combustors," 42nd AIAA Aerospace Sciences Meeting and Exhibit, AIAA Paper 2004-0156, Reno, NV, 2004.

[13] Cai, J., Ichihasi, F., Mohammad, B. S., Tambe, S. B., Kao, Y.-H., and Jeng, S. M., "Gas Turbine Single Annular Combustor Sector: Combustion Dynamics," 48th AIAA Aerospace Science Meeting, AIAA Paper 2010-21, Orlando, Florida, 2010.

[14] Mohammad, B. S., Cai, J., and Jeng, S. M., "Gas Turbine Combustor Flow Structure Control Through Modification of the Chamber Geometry," *Journal of Engineering for Gas Turbines and Power* (accepted for publication); also ASME Paper GTP-10-1317), 2010.

[15] Mohammad, B., Jeng, S., and Andac, G., "Influence of Fuel Injection and Primary Jets on the Aerodynamics of a Prototype Gas Turbine Combustor," *Journal of Engineering for Gas Turbines and Power* (accepted for publication); also ASME Paper GTP-10-1057, 2010.

[16] Stevens, S. J., and Carrotte, J. F., "Experimental Studies of Combustor Dilution Zone Aerodynamics, Part II: Jet Development," *Journal of Propulsion and Power*, Vol. 6, No. 4, 1990, pp. 504–511. doi:10.2514/3.25463

[17] Goebel, S., Abuaf, N., Lovett, J., and Lee, C., "Measurements of Combustor Velocity and Turbulence Profiles," ASME Paper 93-GT-228, 1993.

[18] Holdeman, J. D., "Mixing of Multiple Jets with a Confined Subsonic Crossflow," *Progress in Energy and Combustion Science*, Vol. 19, No. 1, 1993, pp. 31–70. doi:10.1016/0360-1285(93)90021-6

[19] Gulati, A., Tolpadi, A., VanDeusen, G., and Burrus, D., "Effect of Dilution Air on the Scalar Flowfield at Combustor Sector Exit," *Journal of Propulsion and Power*, Vol. 11, No. 6, 1995, pp. 1162–1169. doi:10.2514/3.23955

[20] Anacleto, P., Heitor, M., and Moreira, A., "The Mean and Turbulent Flowfields in a Model RQL Gas-Turbine Combustor," *Experiments in Fluids*, Vol. 22, No. 2, 1996, pp. 153–164. doi:10.1007/s003480050033

[21] Doerr, T., Blomeyer, M., and Hennecke, D., "Optimization of Multiple Jets Mixing with a Confined Crossflow," *Journal of Engineering for Gas Turbines and Power*, Vol. 119, Nos. 315–321, 1997. doi:10.1115/1.2815577

[22] Gritsch, M., Martiny, M., Schulz, A., Kim, S., and Wittig, S., "Gas Turbine Heat Transfer: Newest Developments in Components Performance," *Heat Transfer 1998: Proceedings of the 11th International Heat Transfer Conference (IHTC)*, Kyongju, Korea, Aug. 1998.

[23] Barringer, M., "Design and Benchmarking of a Combustor Simulator Relevant to Gas Turbine Engines," M.S., Thesis, Virginia Polytechnic Institute and State University, Blacksburg, VA, 2001.

[24] Keane, R. D., and Adrian, R. J., "Theory of Cross-Correlation Analysis of PIV Images," *Applied Scientific Research*, Vol. 49, No. 3, 1992, pp 191–215. doi:10.1007/BF00384623

[25] Mohammad, B., and Jeng, S., "Effect of Geometry on the Aerodynamics of a Prototype Gas Turbine Combustor," ASME Turbo Expo Paper GT2010-23082, Glasgow, Scotland, U.K., 2010.

G. Richards
Associate Editor